Developmental Biology 455 (2019) 85–99

Contents lists available at ScienceDirect

Developmental Biology

journal homepage: www.elsevier.com/locate/developmentalbiology

Original research article

Lineage tracing of *col10a1* cells identifies distinct progenitor populations for osteoblasts and joint cells in the regenerating fin of medaka (*Oryzias latipes*)

Manish Dasyani [a,1], Wen Hui Tan [a,1], Sudha Sundaram [a], Nurgul Imangali [a], Lazaro Centanin [b], Joachim Wittbrodt [b], Christoph Winkler [a,*]

[a] Department of Biological Sciences and Centre for Bioimaging Sciences, National University of Singapore, Singapore, 117543, Singapore
[b] Centre for Organismal Studies, University of Heidelberg, 69120, Heidelberg, Germany

ARTICLE INFO

Keywords:
Collagen10a1
Lineage tracing
Regeneration
Medaka
Cell ablation
Transdifferentiation
Osteoblasts
Blastema

ABSTRACT

The caudal fin of teleost fish regenerates fully within two weeks of amputation. While various cell lineages have been identified and characterized in the regenerating fin, the origin of bone cells remains debated. Here, we analysed *collagen10a1* (*col10a1*) expressing cells in the regenerating fin of the medaka (*Oryzias latipes*) and tested whether they represent an alternative progenitor source for regenerating osteoblasts. Under normal conditions, *col10a1* cells are positioned along fin ray segments and in intersegmental regions. Lineage tracing in the amputated fin revealed that *col10a1* cells from the stump contribute to the regenerating bony fin rays. However, ablation of *col10a1* cells did not abolish fin regeneration suggesting that *col10a1* expressing osteoblast progenitors are dispensable for regeneration. Intriguingly, however, after ablation of *osterix* (*osx*)*/sp7-col10a1* double-positive osteoblasts, *col10a1* cells exclusively gave rise to joint cells in the intersegmental region thus identifying a pool of lineage-restricted joint progenitor cells. To identify additional sources for regenerating osteoblasts, we performed clonal lineage analysis. Our data provide the first evidence that after ablation of mature osteoblasts in medaka, transdifferentiation does not account for *de novo* osteoblast generation. Instead, our findings suggest the presence of lineage restricted progenitor pools in medaka, similar to the situation in zebrafish. After osteoblast ablation, these pools become activated and give rise to fin ray osteoblasts and intersegmental joint cells during regeneration. In summary, we conclude that *col10a1*-positive cells do not represent an exclusive source for osteoblasts but are progenitors of joint cells in the regenerating fin.

1. Introduction

Teleost fish and salamanders show remarkable abilities to regenerate lost appendages by forming a blastema underneath the wound epidermis (reviewed in Brockes and Kumar, 2008; Nye et al., 2003). Early studies suggested that the blastema comprises a homogenous population of multipotent cells that give rise to different cell types (Johnson and Bennett, 1999; Poleo et al., 2001). However, subsequently it was shown that the blastema contains heterogeneous populations of lineage restricted progenitor cells (Knopf et al., 2011; Kragl et al., 2009; Lo et al., 1993; Sousa et al., 2011; Stewart and Stankunas, 2012; Tu and Johnson, 2011). A major focus in regeneration studies has been to establish the identity of cells contributing to the blastema. It is widely accepted that differentiated cells at the amputation stump dedifferentiate, enter a progenitor state and contribute to the blastema (Blum and Begemann, 2015; Echeverri et al., 2001; Hay and Fischman, 1961; Lo et al., 1993; Straube and Tanaka, 2006). Interestingly, lineage tracing in newts and axolotls revealed stem cell activation as an additional mechanism for the recruitment of blastema cells (Sandoval-Guzman et al., 2014). Therefore, the characterization of stem and progenitor cells that contribute to a blastema in regenerating appendages requires further analysis.

The teleost caudal fin is an excellent model to study the cellular basis of regeneration. It consists of bony fin rays made up of two parentheses-shaped mineralized dermal bones, the lepidotrichia (reviewed in Akimenko et al., 2003). A single layer of differentiated osteoblasts is positioned along each lepidotrichium (Santamaria and Becerra, 1991). Early osteoblast progenitors in the fin express *runx2a* and *runx2b* (Flores et al., 2004), while intermediate stage osteoblasts express *osterix* (*osx*)*/sp7* and *collagen 10a1* (*col10a1*) (Avaron et al., 2006; Li et al., 2009; Renn et al., 2013). In zebrafish and medaka, mature osteoblasts maintain expression

* Corresponding author. Department of Biological Sciences, National University of Singapore 14 Science Drive 4, S1A-06-07, 117543, Singapore.
E-mail address: dbswcw@nus.edu.sg (C. Winkler).
[1] These authors contributed equally.

https://doi.org/10.1016/j.ydbio.2019.07.012
Received 12 October 2018; Received in revised form 30 June 2019; Accepted 16 July 2019
Available online 17 July 2019

of *osx* and *col10a1* and eventually express late bone markers such as *osteocalcin* (*osc*) (Li et al., 2009; Renn et al., 2013). In teleosts, *col10a1* is expressed in both osteoblasts and chondrocytes (Renn et al., 2013; Smith et al., 2006), while in humans *COL10A1* is expressed exclusively in hypertrophic chondrocytes (Bateman et al., 2004; McIntosh et al., 1995).

How cells in the blastema acquire their osteoblast identity during fin regeneration has been addressed by lineage tracing (Ando et al., 2017; Knopf et al., 2011; Sousa et al., 2011; Stewart and Stankunas, 2012). This showed that in response to amputation mature osteoblasts at the stump detach from the bone surface, dedifferentiate, and start proliferating. These dedifferentiated cells then migrate beyond the amputation plane into the blastema, and generate the osteoblast population in the regenerate without contributing to other cell types (Sousa et al., 2011). However, ablation of differentiated osteoblasts before amputation did not impair the recruitment of new osteoblasts to the regenerate suggesting alternate cellular sources in addition to dedifferentiated osteoblasts (Singh et al., 2012). Transdifferentiation of intra-ray fibroblasts into osteoblasts has been discussed previously (Akimenko et al., 1995; Smith et al., 2006). Conversely, clonal analysis demonstrated lineage restriction in the regenerating fin (Tu and Johnson, 2011). A recent cell-lineage analysis in zebrafish identified *matrix metalloproteinase 9* (*mmp9*) expressing cells as osteoblast progenitor cells (OPCs). These *mmp9* cells reside in the fin ray joints and extensively contribute to osteoblasts of the regenerating fin (Ando et al., 2017). Together with an earlier report that joint cells share their cell lineage with osteoblasts (Sousa et al., 2011; Tu and Johnson, 2011), this establishes the joint regions as an important origin of osteoblast progenitors during regeneration. In the present study, we used transgenic medaka fish to label, lineage trace and ablate joint cells and osteoblasts during regeneration. We show that *col10a1* expression marks two non-interconvertible cell populations in the regenerating medaka fin that give rise to joint cells and osteoblasts, respectively. Based on clonal analysis, we provide evidence that suggests contribution from osteoblast progenitors to the regenerating medaka fin after ablation of differentiated osteoblasts.

2. Material and methods

2.1. Generation and maintenance of medaka lines

Transgenic and wildtype (Cab) medaka were maintained in the fish facility of the Department of Biological Sciences, National University of Singapore (DBS, NUS) in recirculating aquarium systems under a controlled 14/10 light cycle. Breeding and experimental procedures were approved by the Institute of Animal Care and Use Committee of the National University of Singapore (IACUC; protocol numbers: BR15-0119, R14-293, R18-0562). *Col10a1*:nlGFP (Renn et al., 2013) and *osx*:GFP (Renn and Winkler, 2012) transgenic lines were previously described. For cell ablation, several constructs were generated. For *col10a1*:CFP-NTR, the mCherry sequence was released from *col10a1*:mCherry (Renn et al., 2013) and replaced with CFP-NTR, which was PCR amplified from *osx*:CFP-NTR (Willems et al., 2012). For *col10a1*:CFP-NTRo, the NTR-polyA in *col10a1*:CFP-NTR was replaced with NTRo-polyA from *osx*:mCherry-NTRo (kindly provided by K. D. Poss, Duke University, USA; Singh et al., 2012). For *col10a1*:mCherry-NTRo, the constructs *osx*:mCherry-NTRo (Singh et al., 2012) and *col10a1*:mCherry were digested to obtain mCherry-NTRo and a backbone containing the *col10a1* promoter. The fragments were ligated to generate *col10a1*:mCherry-NTRo.

The Gaudí$^{BBW2.1}$, Gaudí^{RSG} and Gaudí$^{Ubiq.iCRE}$ lines for lineage tracing were described previously (Centanin et al., 2014). To generate a *col10a1*:CreER^{T2}-p2a-mCherry driver line, the mCherry-PolyA fragment was released from *col10a1*:mCherry, and a linker containing *BamHI*, *SalI*, *SmaI* and *NotI* restriction sites was generated by annealing two oligonucleotides described before (Willems et al., 2012). The *BamHI* and *NotI* digested linker was then ligated to the vector backbone to generate a *col10a1*:MCS plasmid. In a second step, *col10a1*:MCS was digested with *SacII* and *SalI*. For preparation of the insert, a CreER^{T2}-p2a-mCherry--polyA DNA sequence was PCR amplified from *osx*:CreER^{T2}-p2a-mCherry (kindly provided by G. Weidinger, University of Ulm, Germany; Knopf et al., 2011). The digested vector backbone and PCR amplified insert were ligated to obtain *col10a1*:CreER^{T2}-p2a-mCherry.

For transgenesis, plasmids were injected into one-cell stage medaka embryos using the I-*SceI* meganuclease technique (Rembold et al., 2006). Injected fish were screened for mosaic reporter expression. Positive fish were outcrossed to wildtype fish and germline positive founders were identified. Embryos were screened for stable transgenic expression at 7–12 dpf using a Stereoscopic Zoom Microscope SMZ1000 (Nikon Japan). Positive embryos were raised to maintain stable transgenic lines.

2.2. RNA in situ hybridization and immunohistochemistry

RNA *in situ* hybridization and immunohistochemisty on fin cryosections (20 μm) were performed as previously described (McMillan et al., 2018) with slight modifications. For *in situ* hybridization, after NBT/BCIP staining, slides were counterstained with DAPI (0.25 μg/ml) and mounted in Mowiol 4–88 (Calbiochem). Riboprobes for *evx1* (Debiais-Thibaud et al., 2007), *col10a1* (Renn et al., 2013) and *osx* (Renn and Winkler, 2009) were synthesized as previously described. For immunohistochemistry, rabbit anti-ph3 polyclonal antibody (1:100, Millipore 06–570) and secondary goat anti-rabbit Alexa Fluor 488 (1:500, Abcam ab150077) were used. After antibody staining, slides were counterstained with DAPI (0.25 μg/ml) and mounted in Mowiol 4–88.

2.3. Ablation of col10a1 and osx cells

Cell ablation experiments in medaka were performed as described earlier with minor modifications (Singh et al., 2012; Willems et al., 2012). A metronidazole (Mtz) stock solution (1.5 M in DMSO; Sigma) was freshly prepared and adult fish were kept in 3 mM Mtz solution in fish system water for 24 h. Control fish were treated with fish system water containing 0.2% DMSO. The fish were kept in the dark throughout the duration of treatment. After treatment, the fish were washed with system water and transferred back to the fish system until fin amputation.

2.4. Lineage tracing of osteoblasts

For activation of Cre recombinase to allow recombination, embryos and fish older than 15 dpf were treated with 0.5 μM 4-hydroxytamoxifen (4-HT; Sigma) for 24 h or three consecutive days, respectively. Embryos and fish were kept in the dark throughout the duration of treatment. Embryos were washed with 1X Danieau's solution after treatment while adult fish were washed with fish system water before transferring them back into the system. For clonal analysis, medaka transgenic for *osx*:mCherry-NTRo as well as Gaudí^{RSG}/Gaudí$^{Ubiq.iCRE}$ were treated with 0.5 μM 4-HT for 24 and 72 h at 1, 2, 3 and 15 dpf.

2.5. Fin regeneration analysis

For amputation of the caudal fin, adult medaka fish were anaesthetized using 0.03% Tricaine (Sigma) and placed laterally on a petri-dish (Greiner Bio-One). Amputations were performed at a level just posterior to the first fin ray bifurcation using a sterile scalpel blade (Feather). The fish were then recovered by transferring them back to fish system water. Regeneration was allowed to proceed under controlled temperature and light conditions.

2.6. Imaging and statistical analysis

Tricaine anaesthetized fish were placed on a petri-dish (Greiner Bio-One) for imaging of the caudal fin. The images were taken using a Stereoscopic Zoom Microscope SMZ1000 (Nikon Japan) and the NIS-

elements software. For measurement of the length of fin regenerates, the Fiji ImageJ software was used (Schindelin et al., 2012). The straight line tool was used to draw a line from the amputation plane to the tip of the regenerate. Regeneration in control fish under the same imaging conditions was documented. Graphs showing the lengths of the regenerate vs time were plotted using Microsoft Excel. Error bars were calculated using standard error of the mean. An unpaired Student's t-test was performed to analyse the data.

For imaging of cryosections after *in situ* hybridization and immunohistochemistry, a Nikon Eclipse 90i upright microscope (Nikon Japan) equipped with the NIS-elements software and an Olympus FluoView FV3000 confocal microscope were used. To quantify ablation efficiency and ph3 staining, cell counting was performed on confocal z-stack images in reference to DAPI staining in a region 300 μm proximal to the amputation plane. An unpaired Student's t-test was used for statistical analysis. For fluorescence analysis in embryos and lineage tracing studies in adult fish, *in vivo* imaging was performed using a Leica TCS SP5 X confocal microscope. Images were processed and exported using Bitplane Imaris software version 7.7.1. The images were processed and merged using Fiji ImageJ software version 1.50d and Photoshop CC 2015.

3. Results

3.1. Col10a1 expression marks osteoblasts and joint cells in the medaka fin

Earlier studies reported that *osx* is expressed in a single layer of osteoblasts at the surface of lepidotrichia, while *evx1* is expressed in intersegmental regions in zebrafish (Borday et al., 2001; Dardis et al., 2017; Konig et al., 2017; McMillan et al., 2018; Sims et al., 2009; Ton and Iovine, 2013; Yoshinari et al., 2009). Using RNA *in situ* hybridization on longitudinal sections of regenerating fins at 6 days post amputation (6 dpa), we confirmed that also in medaka, *evx1* is expressed in presumptive and maturing intersegmental joints (brackets in Fig. 1A, top). Importantly, *col10a1* is expressed in a subset of joint cells in the *evx1* domain (light blue arrows in Fig. 1A, middle), but some cells in this domain notably lack *col10a1* transcription (white arrows). *Col10a1* is also expressed in presumptive and maturing osteoblasts that line the emerging lepidotrichia (dark blue and red arrows in Fig. 1A, middle). Next, we generated transgenic medaka lines expressing fluorescence reporters fused to mammalianized nitroreductase (NTRo; Singh et al., 2012) under control of *col10a1* and *osx* promoters to visualize joint cells and osteoblasts *in vivo* during fin development and regeneration. Overall, *col10a1*:mCherry-NTRo expression recapitulates endogenous *col10a1* transcription (Fig. 1A, bottom), however, with some differences that we attribute to protein turn-over rates of the used reporters (i.e. folding time and protein stability). For example, we noted cells with strong *col10a1* transcription that were only weakly positive for the reporter protein (red arrow) on the inside of lepidotrichia. This suggests that these cells only recently started to express *col10a1*. On the other hand, we identified cells with strong reporter expression at the distal end of the blastema where *col10a1* transcription is absent. This suggests residual reporter protein persisting in de-differentiated cells that terminated *col10a1* transcription. Importantly, both endogenous *col10a1* and the used *col10a1* transgenic reporters were expressed in a subset of *evx1* positive cells in presumptive and maturing joints in intersegmental regions (light blue arrows in Fig. 1A). Furthermore, *col10a1*:mCherry-NTRo and *col10a1*:CFP-NTRo transgenic fish showed identical expression suggesting no effect of the used reporter on the expression pattern (Supplementary Figs. S1A and B). We also found that our *osx*:mCherry-NTRo reporter recapitulated endogenous *osx* transcription in pre-mature and mature osteoblasts of the regenerating fin (Fig. 1B). Minor differences in staining again can be attributed to delayed reporter maturation and protein stability. Next, *col10a1*:CFP-NTRo transgenic fish were crossed with *osx*:mCherry-NTRo fish to determine the overlap of *col10a1* driven CFP expression in osteoblasts. As expected, *osx*:mCherry-NTRo was expressed in cells lining the lepidotrichia (Supplementary Figs. S1 and S2) while *col10a1*:CFP-NTRo expression was found in some but not all segmental osteoblasts expressing *osx*:mCherry-NTRo (Supplementary Figs. S1 and S2). In addition, CFP expression was also found in joint cells in the intersegmental regions (Supplementary Fig. S1C-C, arrowheads). Importantly, *col10a1* driven reporter expression was absent from basal epidermal cells but found in a layer of osteoblast progenitor cells lining the emerging lepidotrichia, which turn on *osx* transcription in more proximal regions (Supplementary Fig. S2). Fig. 1C summarizes the cellular composition of the regenerating medaka fin.

To determine *col10a1* promoter activity during joint initiation and maturation, we compared reporter expression in fins of *col10a1*:CFP-NTRo/*osx*:mCherry-NTRo double transgenic fish at juvenile and adult stages. Fin growth in juvenile fish occurs by addition of new segments to the distal ends. Therefore, segments and joints at the distal end are younger than those located more proximally (Haas, 1962). At 35 days post fertilization (dpf), we found CFP expression along the entire perimeter of an intersegmental region in a newly forming joint where *osx*:mCherry-NTRo expression is down-regulated (Fig. 2A-A"; arrowheads). However, more mature joints in proximal regions showed CFP expression only at the ends of an intersegment (Fig. 2B-B"; arrowheads). At 3 months post fertilization (mpf), both proximal and distal joints of the adult fish showed transgene expression resembling the situation of mature proximal joints in juvenile fish (Fig. 2C-D").

3.2. Dynamic col10a1 reporter expression in joint cells during fin regeneration

Next, we analysed transgene expression at different stages of fin regeneration. At 2 days post amputation (dpa), we observed epidermal cells covering the amputation site (Fig. 3A). The regenerate at 2 dpa showed expression of *col10a1*:CFP-NTRo at similar levels as in the region proximal to the amputation plane (Fig. 3A'). By stereomicroscopy, *osx*:mCherry-NTRo expression was not detectable in the regenerate (Fig. 3A" and A'") while confocal imaging detected its expression (compare to Fig. 4C). Strong expression of *osx*:mCherry-NTRo was found in the regenerate at 4 dpa (Fig. 3B"), with *col10a1*:CFP-NTRo expression expanding beyond the *osx*:mCherry-NTRo domain towards more distal regions (Fig. 3B',B"'; asterisk). Even considering different maturation times for the used fluorophores, with a maturation half time of ~ 40 min for mCherry (Khmelinskii et al., 2012), this temporal profile suggests that the activation of *col10a1* precedes that of *osx* in the early regenerate.

Until 4 dpa, expression of *col10a1*:CFP-NTRo and *osx*:mCherry-NTRo appeared uniform across the regenerate. This changed from 6 dpa onwards, when distinct regions along the regenerating lepidotrichia started to show elevated CFP but reduced mCherry expression (Supplementary Fig. S3). These regions, where CFP and mCherry do not overlap, eventually developed into morphologically discernible joints, first visible at 8 dpa (Supplementary Fig. S4). The maturing joints precisely followed the pattern established by CFP and mCherry expressing cells at 6 dpa with strongest CFP expression found in the youngest joints. Intersegmental CFP expression gradually decreased with the maturation of joints (Fig. 3C'). Simultaneously, *osx*:mCherry-NTRo expression was absent from the maturing intersegmental regions (Fig. 3C''). Along segments on the other hand, *osx*:mCherry-NTRo expression was maintained. We conclude that distal regions in the regenerating fin show higher levels of *col10a1*:CFP-NTRo expression and suggest that osteoblast progenitors show activation of *col10a1* prior to *osx*, while mature osteoblasts maintain *osx* expression but downregulate *col10a1*.

3.3. Mature osteoblasts are dispensable for fin regeneration in medaka

Upon fin amputation in zebrafish, osteoblasts in the stump dedifferentiate, proliferate and redifferentiate to new osteoblasts (Knopf et al., 2011). However, cell ablation showed that differentiated osteoblasts are dispensable for fin regeneration in zebrafish (Singh et al., 2012). As the

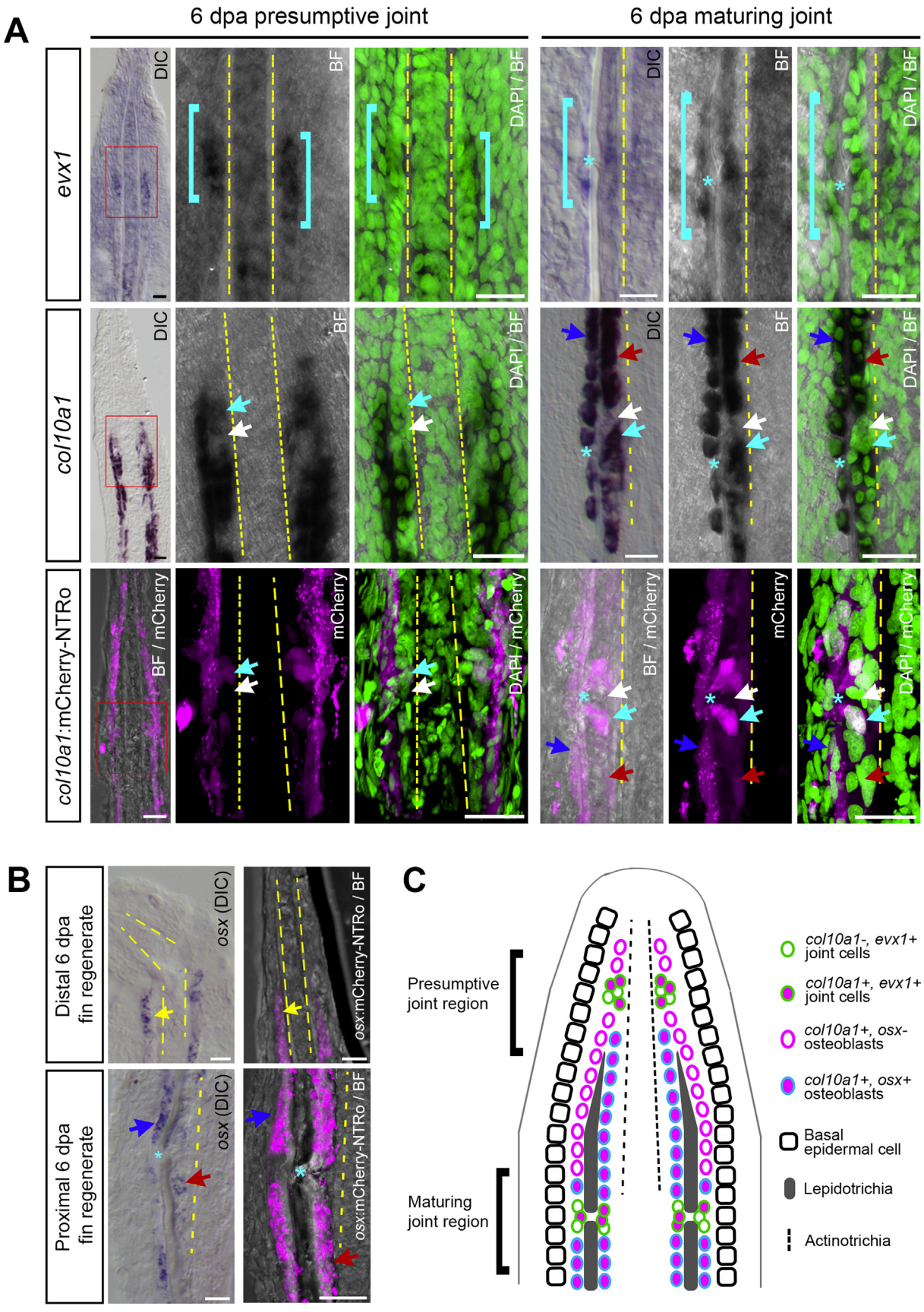

(caption on next page)

Fig. 1. Expression of *evx1*, *col10a1*, *osx*, *col10a1*:mCherry-NTRo and *osx*:mCherry-NTRo in the adult medaka fin. A: Comparison of endogenous *evx1* and *col10a1* expression by RNA *in situ* hybridization and transgenic *col10a1*:mCherry-NTRo expression in the presumptive joint region and maturing joint region of 6 dpa fin regenerates (20 μm longitudinal sections). Endogenous *col10a1* expression and *col10a1*:mCherry-NTRo expression mark a subset of *evx1*-positive joint cells (cyan arrows, n = 3 fin rays, 3 fish). Cyan brackets indicate domains of *evx1*-positive joint cells, asterisks mark joints, yellow dotted lines mark the actinotrichia, cyan arrows mark *col10a1* expression in joint cells, white arrows mark absence of expression in joint cells, dark blue arrows mark the outer row of osteoblasts, red arrows mark the inner row of osteoblasts. **B:** Comparison of endogenous *osx* expression by RNA *in situ* hybridization and transgenic *osx*:mCherry-NTRo expression in distal and proximal regions of 6 dpa fin regenerates (20 μm longitudinal sections). *osx*:mCherry-NTRo expression recapitulates endogenous *osx* expression, marking a single row of osteoblasts (yellow arrows) per hemiray at the distal fin regenerate and two rows of osteoblasts (dark blue and red arrows) per hemiray in the proximal regenerate (n = 3 fin rays, 3 fish). Scale bars = 20 μm. **C:** Schematic diagram indicating expression patterns of *evx1*, *col10a1*, and *osx* in joint cells and osteoblasts at the distal region of a 6 dpa fin regenerate in a longitudinal section view.

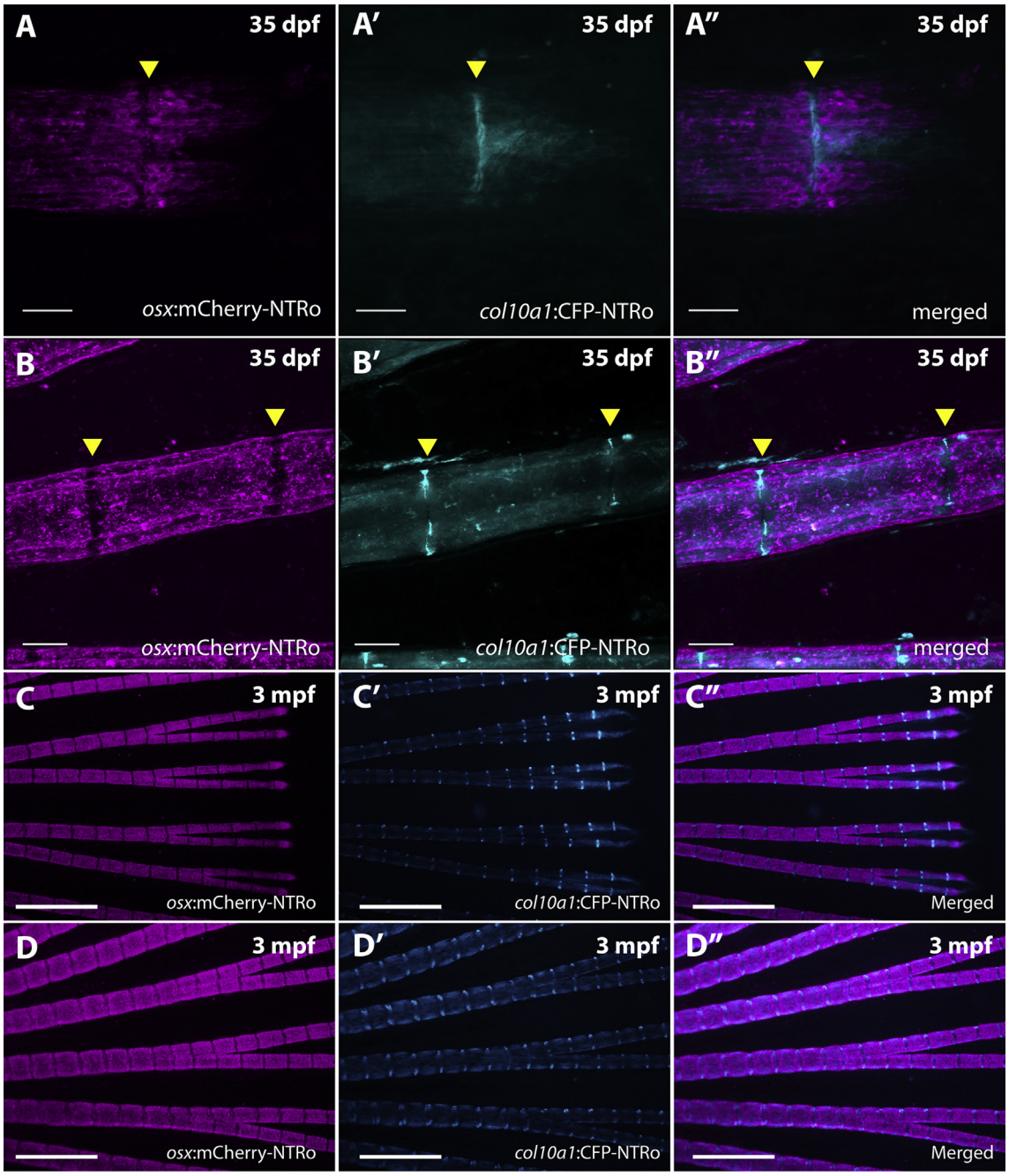

Fig. 2. Expression of *col10a1*:CFP-NTRo and *osx*:mCherry-NTRo in the juvenile and adult caudal medaka fin. A-B: Confocal images of distal (A) and proximal (B) regions in caudal fins of *osx*:mCherry-NTRo/*col10a1*:CFP-NTRo double transgenic medaka at 35 dpf showing mCherry expression in osteoblasts (A,B), CFP expression in osteoblasts and joint cells (A′, B′) and merged images (A″, B″). Scale bars = 40 μm. **C-D:** Distal (C) and proximal (D) regions in caudal fins of *osx*:mCherry-NTRo/*col10a1*:CFP-NTRo double transgenic medaka at 3 mpf. Scale bar = 0.5 mm.

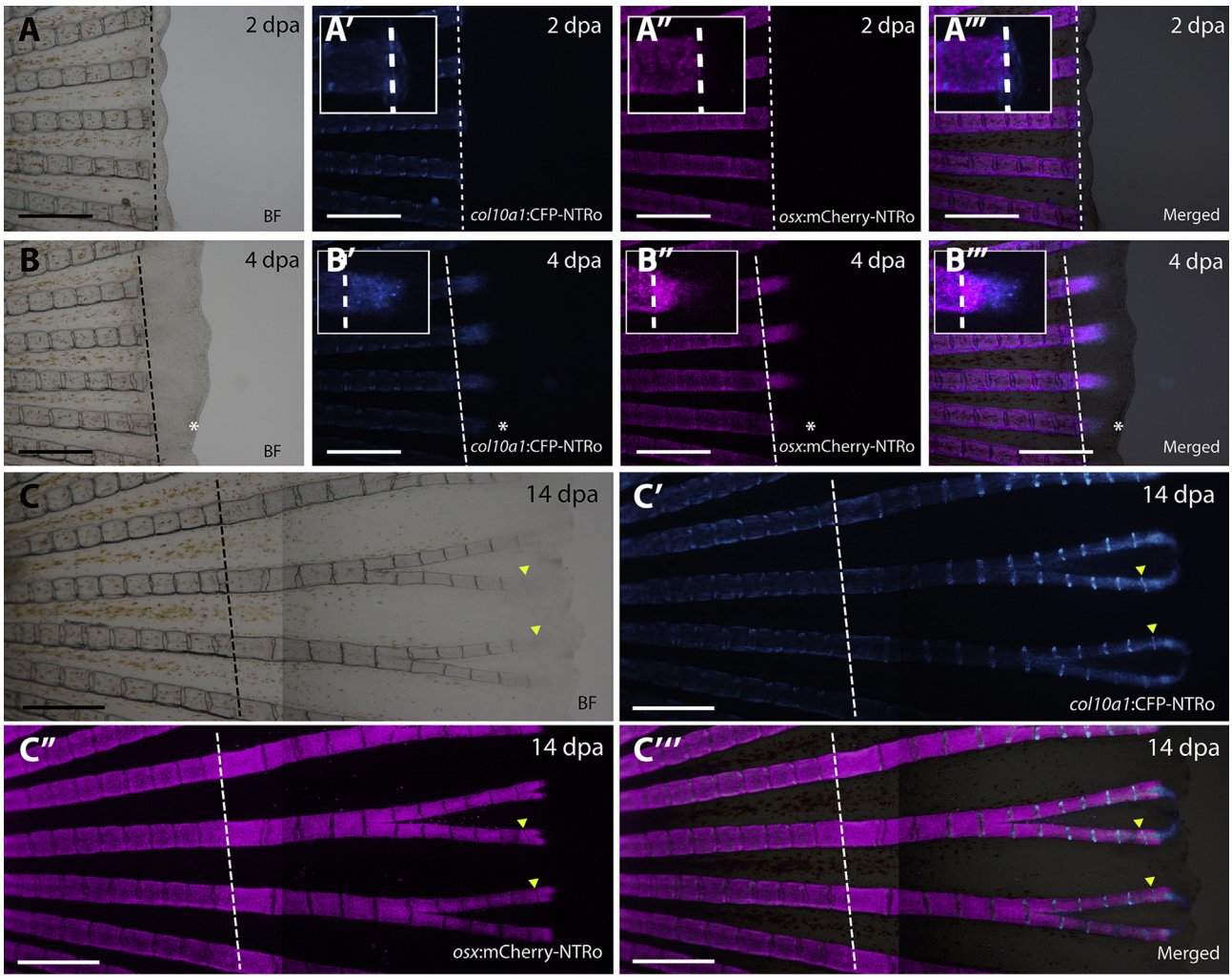

Fig. 3. Expression of *col10a1*:CFP-NTRo and *osx*:mCherry-NTRo during fin regeneration. Images of regenerating fin at 2 (A), 4 (B) and 14 (C) days post amputation (dpa) showing bright field images (A, B, C), CFP expression (A′, B′, C′), mCherry expression (A″, B″, C″) and merged images (A‴, B‴, C′, C‴). Insets in (A,B) show higher magnification views of individual blastema regions indicated by asterisks (in B-B‴). Dotted line indicates amputation plane. Scale bars = 0.5 mm.

source for blastema cells might differ in closely related species (see Sandoval-Guzman et al., 2014), we tested whether osteoblast ablation in medaka has similar effects on fin regeneration as in zebrafish. For this, we used a nitroreductase (NTR) protocol, similar to that described for zebrafish (Singh et al., 2012), however with reduced Mtz concentration to avoid toxicity in medaka. *Osx*:mCherry-NTRo transgenic medaka expressing mammalianized NTRo in osteoblasts were treated with 3 mM Mtz for 24 h followed by fin amputation two days later (Fig. 4A). To determine the effect of ablation of differentiated osteoblasts on fin regeneration and osteoblast recruitment in medaka, we imaged the regenerating fins every alternate day after amputation. Non-treated *osx*:mCherry-NTRo fish showed mCherry expression in osteoblasts covering the bony segments (Fig. 4B). Two days after treatment with 3 mM Mtz for 24 h, the caudal fin was amputated (0 dpa). A significant reduction by 93% in the number of *osx*:mCherry-NTRo expressing cells was evident in treated fins when compared to DMSO controls (Fig. 4B,B' for 0 dpa; quantification in Fig. 4M for 2 dpa) suggesting efficient ablation of *osx* expressing osteoblasts. At 2 dpa, the number of *osx*:mCherry-NTRo cells remained low in the spared, i.e. proximal parts of the fin, while strong expression of *osx*:mCherry-NTRo was observed in the regenerate (Fig. 4C,C′). To exclude that residual *osx*:mCherry-NTRo cells that had escaped ablation contributed to the repopulation of the regenerate by excessive proliferation, we performed a phospho-histone 3 (ph3) staining to label cells in M-phase (Fig. 4D-L). When compared to DMSO controls, no significant difference in the percentage of ph3 positive *osx*:mCherry-NTRo cells (yellow arrows in Fig. 4D'-F′) was observed in Mtz-treated fins (quantification in Supplementary Fig. S5). This strongly suggests that *de novo* differentiation of osteoblasts occurs also in medaka similar to what has been described before in zebrafish (Singh et al., 2012). We found that after *osx* cell ablation, fin outgrowth occurred at a similar rate as in negative control siblings treated with Mtz (Fig. 4N). Thus, like in zebrafish, osteoblast recruitment and fin outgrowth are not affected by ablation of *osx*-expressing osteoblasts in the regenerating medaka fin.

3.4. *Col10a1 expression marks two lineage restricted cell populations*

We previously reported that *col10a1* precedes *osx* expression and labels progenitor populations for osteoblasts in the vertebral column of medaka (Renn et al., 2013). In the regenerating medaka fin, however, the progenitors for osteoblasts and joint cells have not been identified. We therefore tested whether *col10a1* positive cells could serve as a progenitor source for these cell types in the fin. For this, lineage tracing of *col10a1* positive cells was performed before and after ablation of *osx* cells. We generated a transgenic line that expresses inducible Cre recombinase ($CreER^{T2}$) and mCherry, separated by a self-cleaving p2a peptide, under control of the *col10a1* promoter. A founder was identified with mCherry expression in the caudal fin identical to the

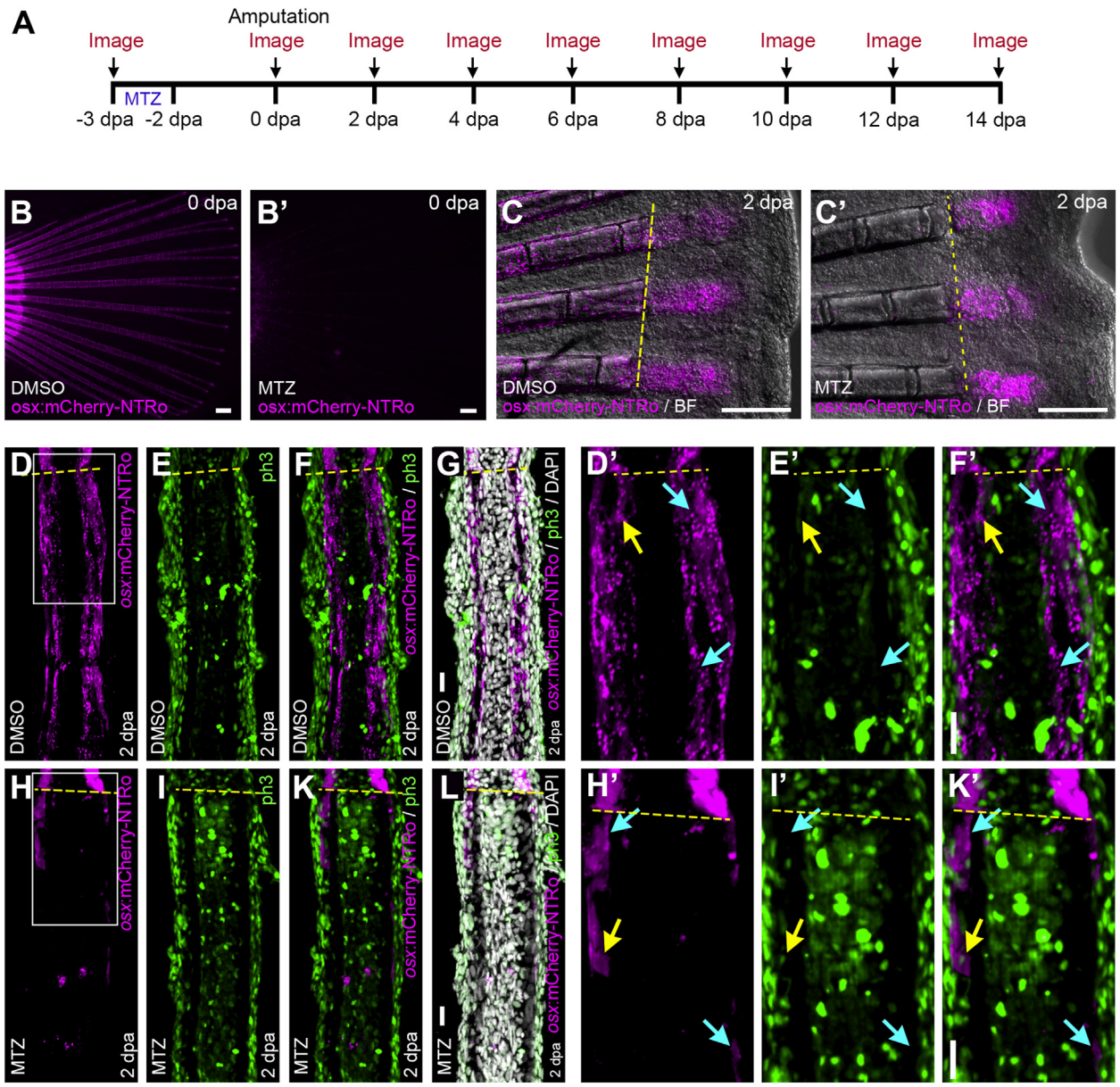

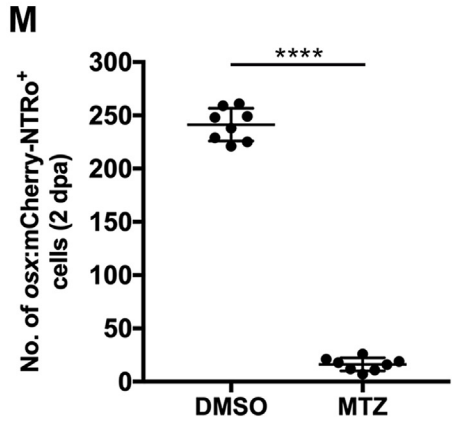

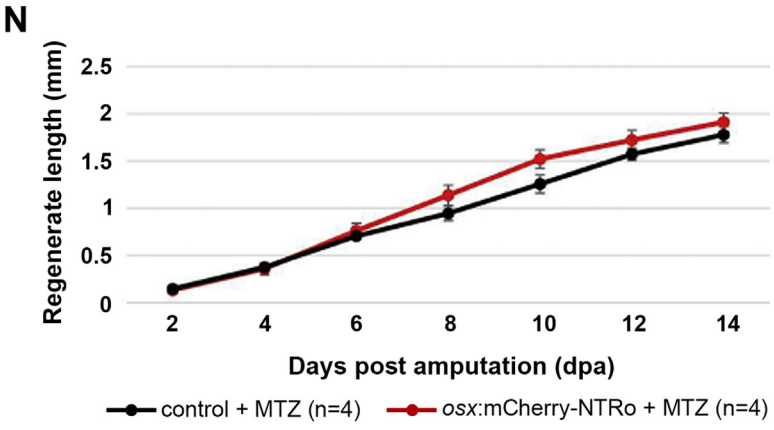

(caption on next page)

Fig. 4. *Osx*:mCherry-NTRo cell ablation in the adult medaka fin does not affect rate of regenerative outgrowth. A. Strategy for ablation of *osx*-positive cells in medaka. Mtz, period of treatment with metronidazole. **B, C:** Transgenic *osx*:mCherry-NTRo fin showing *osx*:mCherry-NTRo expression after DMSO treatment (control; B, C) and Mtz treatment (B′, C′) at 0 dpa and 2 dpa. Scale bars in B, B′, C, C' = 200 μm. **D-L:** ph3 and DAPI staining on 20 μm longitudinal fin sections of DMSO-treated (D-G) and Mtz-treated (H-L) *osx*:mCherry-NTRo fish at 2 dpa. **D′, E′ F′**: Magnified views of the boxed region in (D). **H′, I′, K′**: Magnified views of the boxed region in (H). Yellow dotted lines indicate the amputation plane, yellow arrows indicate mCherry/ph3-double positive cells, cyan arrows indicate mCherry-positive, ph3-negative cells. Scale bars in G, F′, L, K' = 20 μm. **M:** Number of *osx*:mCherry-NTRo-expressing cells (300 μm from the amputation plane) is significantly reduced (93.3%) in Mtz treated fish (16.3 ± 6.1) compared to DMSO controls (241.3 ± 15.3) at 2 dpa. Error bars indicate mean ± s.d. Cell count was performed on confocal z-stack images of 20 μm longitudinal sections, n = 8 fin rays (N = 6 fish). **N:** Lengths of fin regenerates after *osx* cell ablation. Double transgenic *col10a1*:nlGFP/*osx*:mCherry-NTRo (*osx*:mCherry-NTRo) and *osx*:mCherry-NTRo negative siblings (control) treated with Mtz show similar rates of fin outgrowth. Data are represented as mean ± SEM. Changes are not significant.

col10a1:mCherry-NTRo and *col10a1*:CFP-NTRo lines described above (Supplementary Fig. S1).

For labelling and lineage tracing of *col10a1* cells, *col10a1*:CreER^{T2}-p2a-mCherry transgenic fish were crossed with either the Gaudí$^{BBW2.1}$ or Gaudí^{RSG} *loxP* reporter line (Centanin et al., 2014). Double transgenic *col10a1*:CreER^{T2}-p2a-mCherry/Gaudí$^{BBW2.1}$ fish showed ubiquitous expression of membrane-tagged CFP with mCherry expression restricted to osteoblasts and joint cells of the caudal fin (Supplementary Fig. S6), while Gaudí^{RSG} fish showed ubiquitous DsRed expression (data not shown). *Col10a1*:CreER^{T2}-p2a-mCherry/Gaudí^{RSG} fish were treated with 4-hydroxytamoxifen (4-HT) to activate Cre and trigger recombination at the *loxP* sites in order to randomly label subsets of *col10a1*-positive cells with nuclear-tagged EGFP (Fig. 5A). After recombination and removal of 4-HT, labelled cells were detected in the proximal fin region along bone segments (arrows) and in joints (asterisks) before and after amputation (Fig. 5B-B'' and C-C'', respectively). After amputation, regenerates were imaged every two days to determine the distribution of labelled cells. Substantial numbers of labelled cells were observed in the regenerating fin rays (Fig. 5D-D'''). These numbers increased over time suggesting that the cells undergo extensive proliferation (data not shown). Closer observation revealed that the labelled *col10a1* cells contributed to both segmental osteoblasts and intersegmental joint cells (arrows and arrowheads, respectively, in Fig. 5D'-D''', n = 14 fin rays, 5 fish). Thus, *col10a1* cells in the proximal fin region migrate beyond the amputation plane and contribute to joint cells as well as segmental osteoblasts during regeneration.

To exclude that recombination occurred unintentionally during regeneration driven by residual 4-HT that was not completely removed, we quantified the number of labelled cells in several fin rays at 0 and 8 dpa. Importantly at 8 dpa, we only observed labelled cells in those rays that had been positive also before amputation (at 0 dpa; 17 fin rays analysed in 5 fins). In case of residual 4-HT and random cell labelling post amputation, labelled cells should have occurred also in rays that did not have positive cells at 0 dpa. We never observed such cases (10 fins analysed; data not shown). This shows that 4-HT was effectively removed. Interestingly, not all fin rays that were labelled at 0 dpa gave rise to labelled cells in regenerated rays at 8 dpa (7 fin rays in 3 fins analysed), but the majority did (17 fin rays in 5 fins).

As reported earlier, joint cells and osteoblasts share their progenitors (Ando et al., 2017; Tu and Johnson, 2011). Thus, we asked whether *col10a1*-positive but *osx*-negative (*col10a1+/osx-*) cells found in joints could serve as source for osteoblasts during fin regeneration. For this, we generated a triple transgenic line (Gaudí$^{BBW2.1}$/*col10a1*:-CreER^{T2}-p2a-mcherry/*osx*:mCherry-NTRo) and tracked labelled *col10a1* cells after ablation of *osx* positive osteoblasts. For this, triple transgenic fish were treated with 4-HT to activate Cre and label individual *col10a1* cells with mYFP or nlsEGFP. *Osx* expressing osteoblasts - notably including *col10a1/osx* double positive cells - were ablated 4 days later, and fin amputation was carried out two days after ablation (Fig. 5E). Intriguingly, we found no contribution of labelled *col10a1* cells to the re-emerging pool of *osx* cells in the regenerating segments (Fig. 5F',G'; n = 10 fin rays in 4 independent fish). Instead, labelled *col10a1* cells exclusively populated the intersegmental joint regions (Fig. 5F'',G''; Supplementary Fig. S7). This suggests that *col10a1* marks two pools of progenitor cells: one pool represents *col10a1/osx* double-positive cells that contribute to osteoblasts of the regenerating segments; the second pool consists of *col10a1+/osx-* cells in the intersegmental regions that contribute exclusively to joint cells in the regenerate.

3.5. *col10a1 expressing progenitors are dispensable for fin regeneration*

After we demonstrated that *col10a1* cells contribute to segments and intersegmental regions of the regenerate, we wanted to know whether *col10a1* cells act as an alternative cellular source to replace dedifferentiating mature *osx* osteoblasts. For this, we tested the effect of *col10a1* cell ablation on fin regeneration. *Col10a1*:mCherry-NTRo transgenic fish were treated with 3 mM Mtz for 24 h followed by fin amputation (Fig. 6; same settings as in Fig. 4A). After Mtz treatment, mCherry expression was strongly reduced in the stump indicating efficient ablation of *col10a1* cells (Fig. 6A-B''; for *col10a1*:CFP-NTRo ablation efficiency see Supplementary Fig. S8). At 2 dpa, mCherry expressing cells appeared in the blastema suggesting that *col10a1* ablation did not affect the recruitment of *de novo* formed *col10a1* osteoblasts in the regenerate (Supplementary Fig. S9). At 4 dpa, newly formed *col10a1* cells populated the presumptive intersegmental regions in the regenerating fin (Fig. 6B-B''; arrowheads). With further outgrowth, the recruitment of *col10a1* cells to distal segments and intersegmental regions remained not affected by *col10a1* ablation (Supplementary Fig. S9), similar to the situation in non-ablated fins. We found no significant difference in the rate of fin outgrowth after ablation as compared to control siblings treated with Mtz (Fig. 6C). This shows that pre-existing *col10a1* cells are dispensable for recruitment of osteoblasts and joint cells in the regenerate.

3.6. *Simultaneous ablation of col10a1 and osx cells slows down regeneration*

Dedifferentiation of *osx*-positive osteoblasts, as proposed by Knopf et al. (2011), could explain normal fin outgrowth in *col10a1* ablated fins. Thus, we asked whether simultaneous ablation of both *col10a1* and *osx* cells affects bone cell recruitment and regeneration. *Col10a1*:CFP-NTRo/*osx*:mCherry-NTRo double transgenic fish were treated with 3 mM Mtz for 24 h and fin amputation was performed at 2 dpt (0 dpa; Fig. 7; same settings as in Fig. 4A). After amputation, CFP expression started to appear in the blastema of regenerate from 2 dpa onwards, preceding mCherry expression in osteoblasts (Supplementary Fig. S10), similar to the situation in non-ablated fins (Fig. 3A'-A'''). At 4 dpa, *osx* expressing osteoblasts appeared along with *col10a1* cells in the regenerate while the spared, i.e. proximal, region showed absence of *osx* and *col10a1* cells (Fig. 7B-B'''). At 14 dpa, *osx* cells spanned the length of regenerated bone segments while *col10a1* cells predominantly localized to the joint regions (Fig. 7C-C'''; arrowheads). Although osteoblasts and joint cells appeared to form normally after simultaneous *osx* and *col10a1* cell ablation, we noticed a significant reduction (19%) in the rate of fin outgrowth in the ablated fins (average length 1.84 ± 0.2 mm) compared to wildtype controls treated with Mtz (2.25 ± 0.12 mm, p = 0.0001; Fig. 7D). This shows that simultaneous ablation of mature osteoblasts and *col10a1* progenitors slows down regeneration but does not prevent it entirely. While this observation is consistent with a contribution of both cell types to regeneration, it also suggests the presence of alternative sources for *de novo* formed osteoblasts and joint cells.

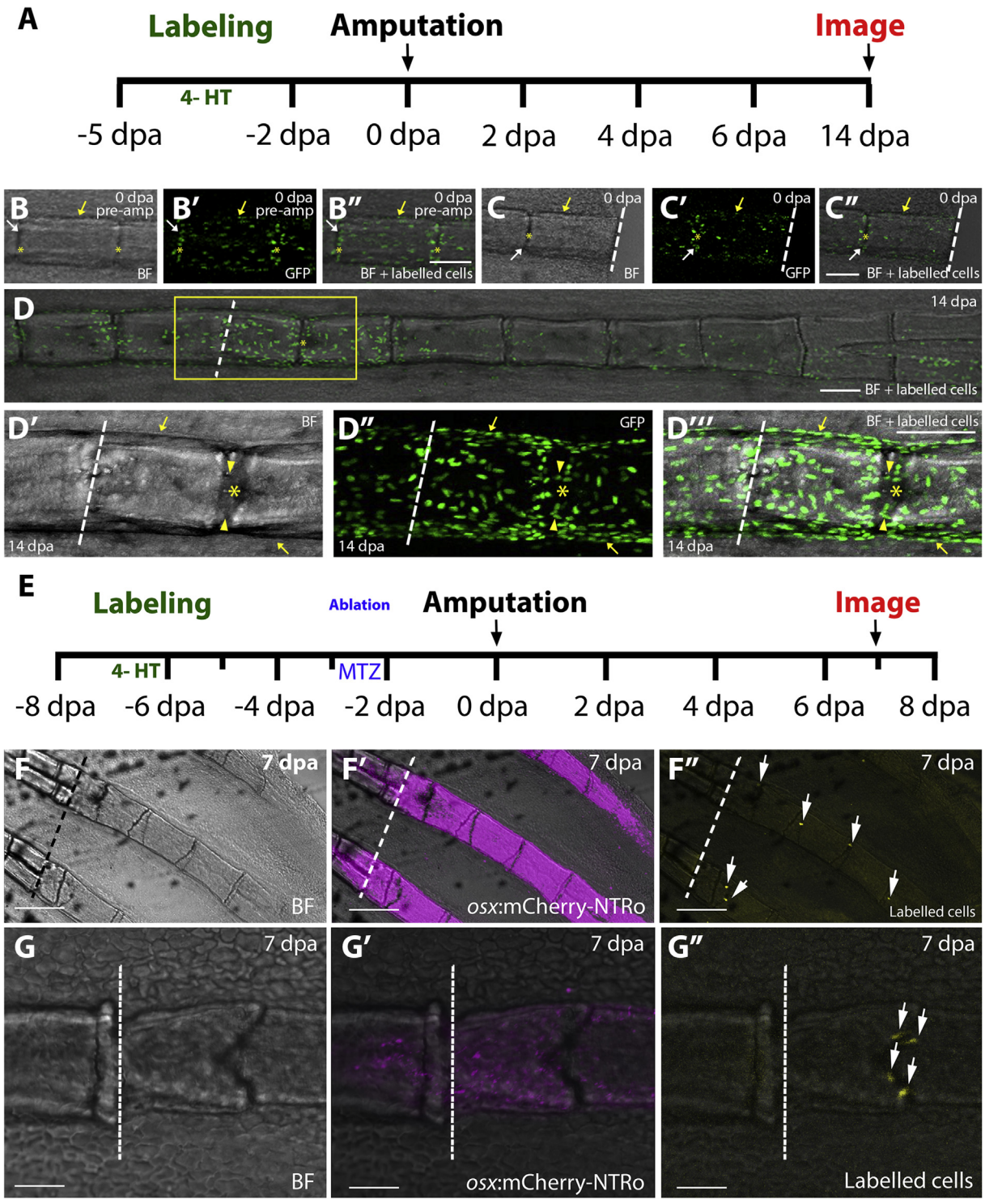

Fig. 5. Contribution of *col10a1* cells to the regenerating fin. A: Strategy employed for Gaudi (Cre-loxP)-mediated lineage tracing of *col10a1* cells in the regenerating fin. Cre-induced recombination is triggered by incubating fish in 4-hydroxytamoxifen (4-HT) for three days starting at -5 dpa. **B-C:** Confocal images of GFP-labelled *col10a1* cells in Gaudi^{RSG} fish at 0 dpa, before amputation (B, B′, B″) and after amputation (C, C′, C″). White arrows indicate labelled joint cells, yellow arrows indicate labelled segmental cells. **D-D‴:** Overview (D) and magnified confocal images of boxed region (D′-D‴) showing contribution of labelled *col10a1* cells to segments (arrows, bone lining cells) and intersegmental joint regions (arrowheads) at 14 dpa (n = 14 fin rays, 5 fish). Asterisks indicate joints, dotted lines indicate the amputation plane. Scale bars = 100 μm. **E:** Strategy employed for *col10a1* cell lineage tracing after *osx* cell ablation. **F-G:** Overview (F; scale bars = 200 μm) and magnified confocal images (G; scale bars = 50 μm) of re-emerged *osx*:mCherry-NTRo cells (F′, G′) and YFP labelled *col10a1* cells (F″, G″) at 7 dpa showing contribution of labelled cells exclusively to joints (arrows). Dotted lines indicate the amputation plane. BF = brightfield.

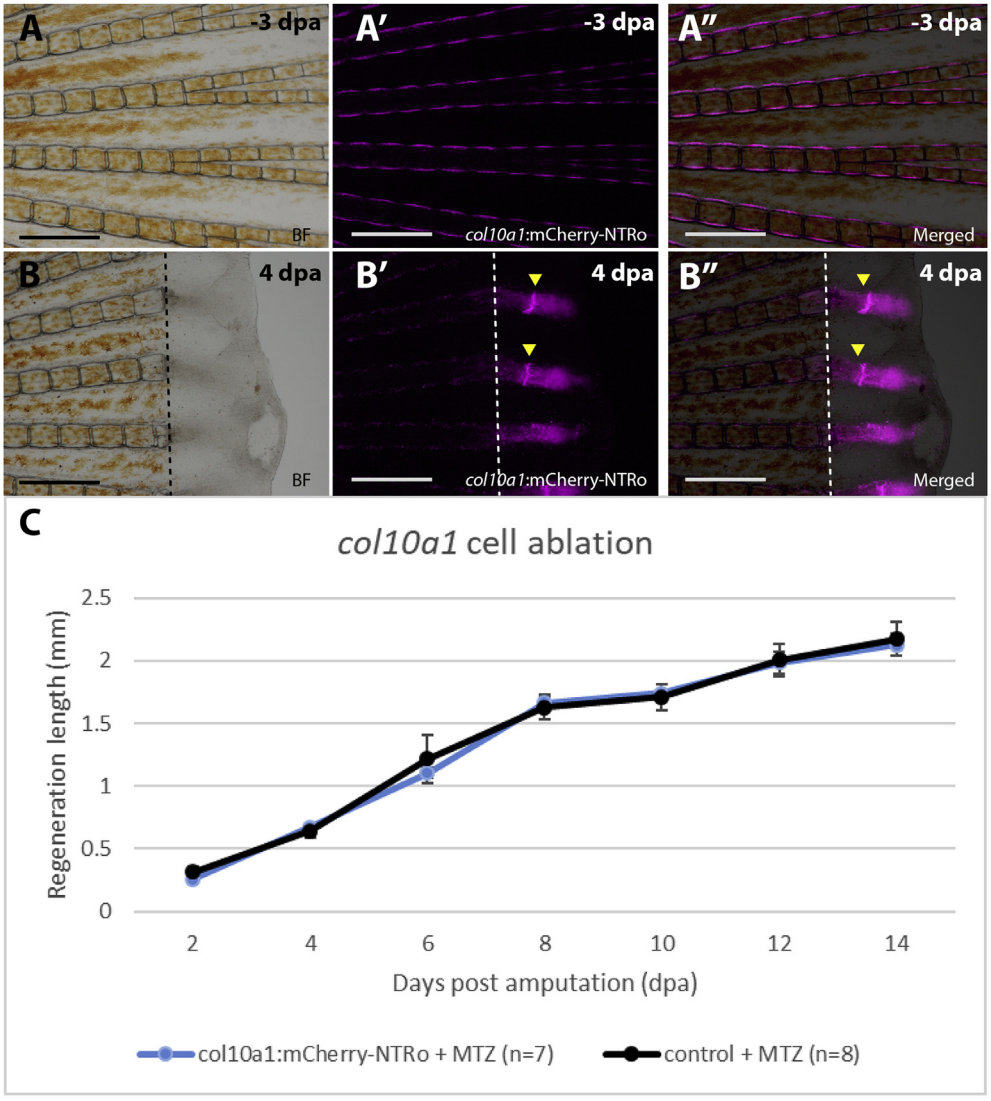

Fig. 6. Fin regeneration after *col10a1* cell ablation. A,B: Images of fins before treatment (A) and regenerates at 4 dpa (B) showing bright field (A,B), *col10a1*:mCherry-NTRo expressing cells (A′,B′) and merged images (A″,B″). Arrowheads indicate *col10a1*:mCherry-NTRo positive cells in the regenerating intersegmental region. Scale bars = 0.5 mm. **C:** Average lengths of regenerates at different time points. *Col10a1* cell ablated fish show a similar rate of fin regeneration as compared to control siblings treated with Mtz. Data are represented as mean ± SEM.

3.7. Lineage restricted progenitor pools act as source for osteoblasts after osx cell ablation

There are at least two mechanisms that could explain supply of newly formed osteoblasts in the regenerate in response to osteoblast ablation, namely stem cell activation and transdifferentiation. To address which mechanism is in place we adopted a strategy previously described by Tu and Johnson (2011), and randomly labelled cell clones during embryonic development to identify 'organ founding stem cells' (FSCs; see Tu and Johnson, 2011). The labelled cells were then traced after *osx* ablation to identify possible sources for osteoblasts. To label different FSCs, triple transgenic *osx*:mCherry-NTRo/Gaudí^{RSG} /Gaudí$^{Ubiq.iCRE}$ medaka with ubiquitous expression of inducible Cre and *loxP* flanked reporters were treated with 4-HT at 1 to 15 dpf. Embryos with labelled cells were raised and adults were sorted at 3 mpf to identify mosaic fish (n = 50) with nuclear tagged H2B-EGFP-positive clones in different cell types of the fin derived from labelled FSCs (Fig. 8A).

We divided the mosaics into three types depending on the position of labelled cells in the fins with respect to segmental osteoblasts expressing *osx*:mCherry-NTRo (Fig. 8B-E″). As expected, most fin rays showed a combination of different labelled cell types. Mosaics with cells positioned lateral to segmental osteoblasts were classified as Type I and were identified in 22 out of 33 analysed fin rays (66.67%; 25 fish analysed; Fig. 8B). Only nine out of these 22 fin rays exclusively had labelled Type I cells. The remaining 13 fin rays in addition had cells of other types (Type II or Type III, or both) as described below (and in Fig. 8C and D). Previous studies reported that all fin cell types, except epidermal and blood cells, extend distally along individual fin rays suggesting the presence of distinct post-embryonic FSCs that contribute to individual fin rays (Tu and Johnson, 2010). Importantly, Type I cells were not limited to individual fin rays but found in patches spread across several rays. This is consistent with the idea that Type I cells possibly represent epidermal cells. Together with joint cells, EGFP-labelled osteoblasts that express *osx*:mCherry-NTRo in segmental regions (Fig. 8E", arrows), were classified as Type II mosaics. Type II mosaics were found in 9 out of 33 analysed fin rays (27.27%) out of which only three were exclusive for Type II cells. Type II mosaics showed EGFP cells also in the intersegmental region (Fig. 8E", asterisk) confirming that the same FSC population gives rise to segmental osteoblasts and joint cells. Type III mosaics were classified based on their position in the intra-ray region, in a focal plane that is medial to segmental osteoblasts. This intra-ray region contains several cell types including dermal fibroblasts, glia and endothelial cells of arteries and veins (Tu and Johnson, 2011). We hence divided Type III mosaics into two sub-classes: Type IIIa mosaics were identified in 13 fin rays and comprise labelled cells not associated to blood vessels (Fig. 8C). Type IIIb mosaics, identified in three fin rays, likely represent endothelial cells lining arteries and veins, based on their morphology and position (Fig. 8D). These mosaics, like for Type II, showed labelled clones only

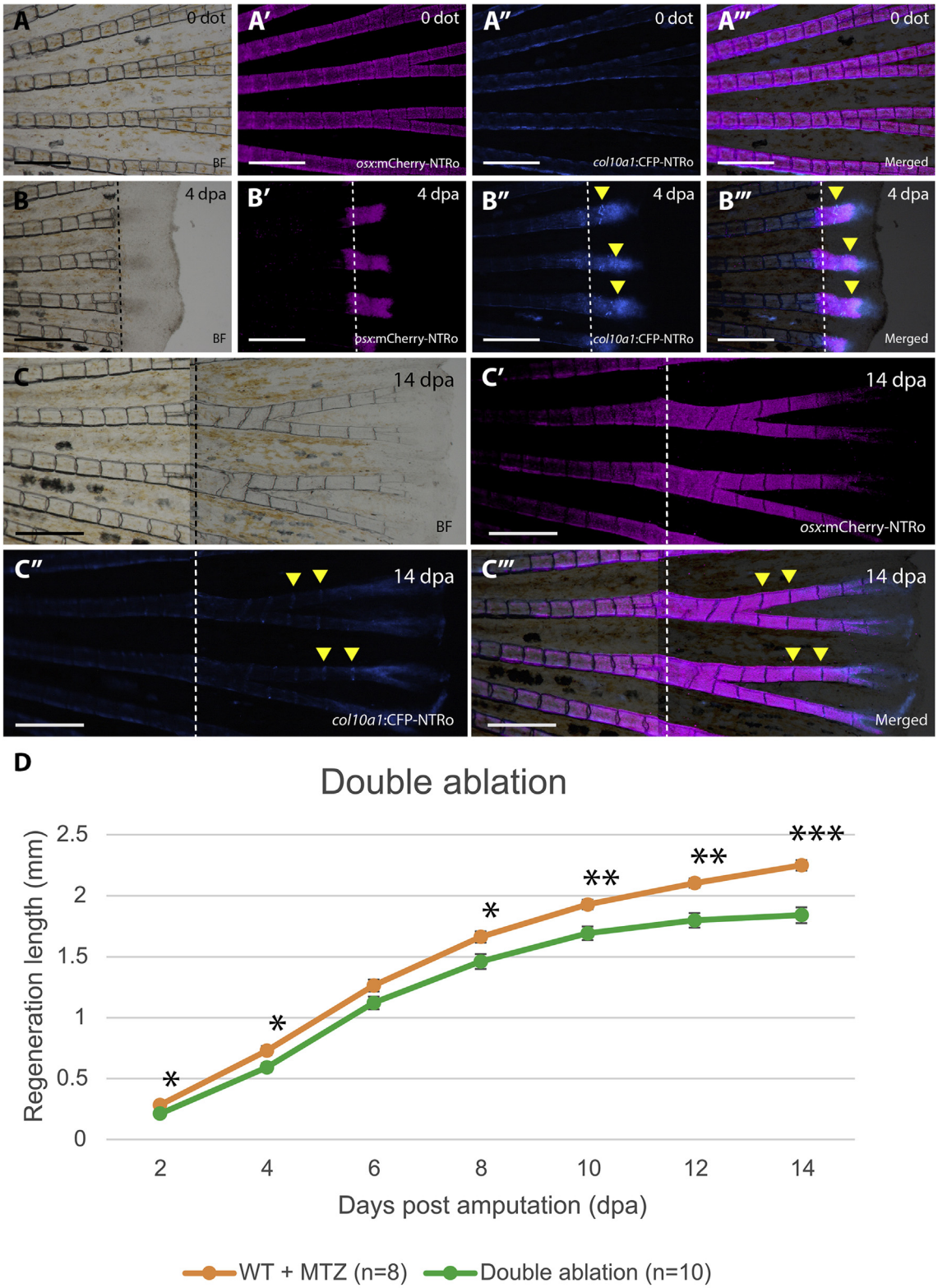

Fig. 7. Fin regeneration after double ablation of *osx* and *col10a1* cells. A,B: Images of fins before double ablation (A) and in regenerates at 4 dpa (B) showing bright field (A,B), *osx*:mCherry-NTRo (A′,B′), *col10a1*:CFP-NTRo (A″,B″), as well merged images (A‴,B‴). Dotted lines indicate amputation planes. Scale bars = 0.5 mm. **C:** Fins at 14 dpa. Image arrangement as in A and B. **D:** Length of fin regenerates after double ablation of *osx* and *col10a1* cells. At 14 dpa, fins depleted of *osx* and *col10a1*-positive cells show a 19% reduction in the length of regenerates as compared to wild-type control fish treated with Mtz (*$P < 0.05$; **$P < 0.005$; ***$P < 0.0001$). Data are represented as mean ± SEM.

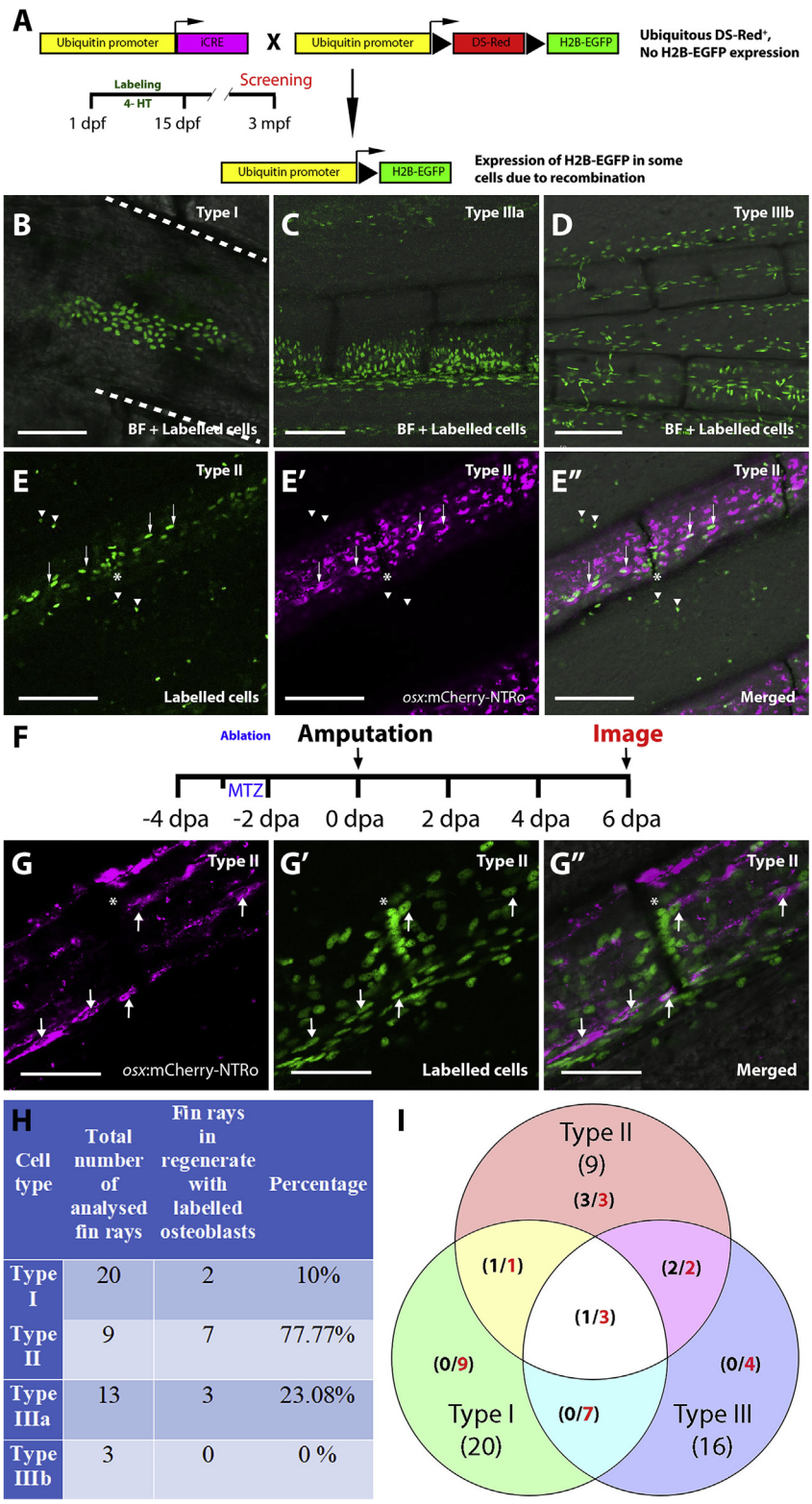

H

Cell type	Total number of analysed fin rays	Fin rays in regenerate with labelled osteoblasts	Percentage
Type I	20	2	10%
Type II	9	7	77.77%
Type IIIa	13	3	23.08%
Type IIIb	3	0	0 %

Fig. 8. Lineage tracing of randomly labelled cells identifies sources for osteoblast regeneration. A: Strategy for labelling different cell lineages by 4-HT incubation at embryonic and post-hatching stages (1 – 15 dpf) and detection of labelled cells in the adult fin (3 mpf). Triangle represents *loxP* sites. **B-E″**: Confocal images of adult fins at 3 mpf showing labelling of different cell types (identities were predicted based on position and morphology; see Tu and Johnson, 2011): Type I (epidermal and blood cells, B), Type IIIa (intraray fibroblasts; C) and Type IIIb (endothelial cells; D). The panel in E shows Type II cells (osteoblasts) that co-express *osx*:mCherry-NTRo (E′), as evident in merged image (E″; EGFP, mCherry and brightfield merged images). Dashed white lines in B indicate borders of fin rays. Arrowheads indicate GFP signal outside the fin rays of unclear origin. Scale bars = 100 μm. **F:** Timeline for *osx* cell ablation, amputation and imaging of labelled cells in the regnerating fin. **G:** Representative confocal images showing *osx*:mCherry-NTRo expressing osteoblasts (G), lineage traced type II cells (G′), and merged image at 6 dpa. Note *osx* expression in some of the labelled cells (arrows). Asterisks label the intersegmental regions. Scale bars = 100 μm. **H,I:** Table (H) and Venn diagram (I) showing contribution of different classes of labelled cells (Types I to III) to the osteoblast lineage. Numbers in red indicate total number of fin rays positive for particular cell type, numbers in black indicate fin rays with contribution to osteoblasts (after ablation) per number of analysed fin rays.

along individual fin rays. Out of a total of 16 Type III labelled fin rays, only four were exclusive for Type III. Thus, mixtures of Types I to III were often observed in the analysed fin rays and Types I, II and III were rarely exclusive (Fig. 8I).

Next, to test whether alternative sources account for *de novo* osteoblast formation after ablation of mature osteoblasts, we followed the fate of individual clones in each fin ray after ablation of *osx*:mCherry-NTRo cells and amputation (Fig. 8F). Fin rays in the regenerated fins were imaged at 6–8 dpa to determine if cells identified as Types I to III contribute to segmental *osx*:mCherry-NTRo expressing osteoblasts (Fig. 8G, arrows) as well as cells in the intersegmental regions (Fig. 8G, asterisk). 2 out of 20 analysed fin rays (10%) from the group of Type I mosaics showed labelled osteoblasts in the regenerate (Fig. 8H). On the other hand, 7 out of 9 Type II mosaics showed contribution to the

osteoblast pool. Finally, 3 out of 13 Type IIIa and none of the Type IIIb labelled clones showed contribution to regenerated osteoblasts (Fig. 8H). Importantly, all fin rays showing labelled osteoblasts in the regenerate included a contribution from Type II mosaics, and none of the pure Type I or III mosaics ever contributed to osteoblasts (Fig. 8I). This suggests that under conditions of osteoblast ablation, a transdifferentiation from Type I or III clones into osteoblasts is unlikely. Instead, distinct FSCs or progenitor pools exist that give rise to osteoblasts and joint cells in the regenerating fin after ablation of differentiated osteoblasts.

4. Discussion

Regeneration in vertebrates exhibits significant variations in different species (Sandoval-Guzman et al., 2014). Even among teleosts, extent and mechanisms of regeneration vary in different species. For example, zebrafish and medaka show significant differences in heart and retina regeneration (Ito et al., 2014; Lai et al., 2017; Lust and Wittbrodt, 2018). Therefore, it is important to analyse and compare fin regeneration in both zebrafish and medaka to elucidate similarities and possible differences during the recruitment of cells into the blastema.

In this study, we used lineage tracing and genetic cell ablation to identify sources for osteoblasts and joint cells in the regenerating medaka fin. Previous studies in zebrafish have shown that ablation of mature osteoblasts does not abolish regeneration (Singh et al., 2012). Thus, in addition to osteoblast dedifferentiation (Knopf et al., 2011), alternative progenitor cell populations act as source for *de novo* generated osteoblasts, and these progenitors have recently been identified as *mmp9* positive cells in the joint regions of fin rays (Ando et al., 2017). We characterized *mmp9* in medaka but were unable to detect its expression in the fin (data not shown), suggesting that it might not serve as a suitable progenitor marker in this species. Instead, we had earlier described *col10a1* expressing cells as progenitors for *osx* osteoblasts in the vertebral column (Renn et al., 2013). Therefore, we wanted to test whether *col10a1* cells serve as cellular source for fin regeneration, in particular under conditions when mature osteoblasts had been ablated. Using lineage tracing, we show that *col10a1* cells contribute to joint cells and osteoblasts in the regenerating fin. However, ablation of *col10a1* cells has no effect on fin regeneration, suggesting that these cells are likely generated from of a multipotent progenitor population. Whether in medaka, this progenitor pool is located in the joints, as described for zebrafish (Ando et al., 2017), remains unknown. Interestingly, in this respect, we did observe a few *osx*:mCherry-NTRo negative Type II cells along the hemirays and in intersegmental regions (Fig. 8E). We speculate that these cells could include potential FSCs and their derivatives, but this requires further analysis. Importantly, we find that *col10a1* expression marks a cell population in the joint region that exclusively gives rise to joint cells of the regenerating fin. Furthermore, our clonal analysis suggests that after ablation of mature osteoblasts, transdifferentiation does not contribute to *de novo* osteoblast formation in medaka, consistent with findings in zebrafish (Tu and Johnson, 2011).

4.1. Characterization of osteoblasts in the regenerating medaka fin

We analysed the dynamics of *col10a1* and *osx* cells in the juvenile, adult and regenerating caudal fin of transgenic medaka. First, we confirmed that endogenous *col10a1* is expressed in joint cells and segmental osteoblasts. Further in transgenics, osteoblasts along the bone matrix were found positive for *col10a1* and *osx* driven reporter expression, which is consistent with previous studies (Li et al., 2009; Smith et al., 2006). Maturing osteoblasts in fin segments showed a reduction of *col10a1* promoter activity while *osx* remained active. This suggests that *col10a1* and *osx* have overlapping expression in intermediate stage osteoblasts but not mature osteoblasts, where only *osx* persists. Previously, a systematic expression analyses of different osteoblast markers during zebrafish fin ray regeneration showed that *osx* and *col10a1* osteoblasts align at the tip of amputated lepidotrichia as early as 24 h post amputation (Sousa et al., 2011). In contrast, in medaka, we observed *col10a1* but not *osx* cells in a distal domain of the regenerate at 2 dpa. Our data therefore support earlier findings of *osx*-negative dedifferentiated osteoblasts at the amputation site (Stewart and Stankunas, 2012).

Prospective joint cells in intersegmental regions were visualized by *col10a1*-driven reporter expression. Using this reporter line, we found similar dynamic patterns in developing and regenerating fins. Newly forming distal joints showed expression spanning the entire perimeter of an intersegmental region while mature joints only showed expression at the dorsal and ventral ends. Such a pattern could be explained by differentiation of cells into mature *col10a1*-negative joint cells or the death of *col10a1* cells in the middle of the joint region. Our cell lineage analysis clearly supports the first scenario. We counted *col10a1* lineage-labelled GFP-positive cells that are positioned in the middle region of joints. No such labelled cells should be evident if cell death of *col10a1* cell occurred, while labelled cells should be detectable if they differentiated and became *col10a1* negative. Consistent with the latter case, we observed 15/33 (45%) proximal joints that had GFP-labelled cells in the middle of the matured joints (at 14 dpa; 11 fin rays; 5 fish; Fig. 5D and data not shown).

Not much is known about the mechanism underlying joint formation in the caudal fin. Joint cells share the same progenitors with segmental osteoblasts (Tu and Johnson, 2011), but their extracellular matrix remains non-mineralized. Expression of *evx1* has been reported in intersegmental regions of the zebrafish caudal fin (Borday et al., 2001; Dardis et al., 2017), and its expression pattern is similar to that of *col10a1*. Cytological studies identified *evx1* expressing cells as a subpopulation of Zns-5 positive scleroblasts (Borday et al., 2001; Sims et al., 2009). Here, we show that also in medaka *evx1* is expressed in presumptive and maturing joints. *Col10a1* expression, on the other hand, has been reported in chondrocytes of teleosts (Avaron et al., 2006; Renn et al., 2013), and the zebrafish co-ortholog *col10a1b* is expressed in intersegmental regions (Ton and Iovine, 2013). Recent studies on facial joints formation reported a mechanism by which chondrocytes are maintained in an immature state (Askary et al., 2015). Here, we describe that *col10a1* is expressed in most but not all *evx1* positive joint cells. We speculate that *col10a1* positive cells in the intersegmental regions represent immature chondrocyte-like cells that share the same progenitors with osteoblasts but do not differentiate into *osx*-expressing osteoblasts. We hypothesize that the extracellular matrix produced by *col10a1* cells has particular structural and mechanical features that keep it non-mineralized and flexible. Our reporter lines are useful tools to visualize mechanical constraints of joint cells in future studies.

4.2. The cellular sources for osteoblasts and joint cells in the regenerating fin

In zebrafish fin regeneration, mature osteoblasts at the stump dedifferentiate to generate progenitors that contribute to the blastema (Knopf et al., 2011; Sousa et al., 2011; Stewart and Stankunas, 2012). The ablation of mature osteoblasts in zebrafish, however, did not impair or slow down fin outgrowth showing that *osx* osteoblasts are dispensable and osteoblasts are generated *de novo* (Singh et al., 2012). Here, we show that in medaka *osx* cell ablation also does not eliminate regeneration. Likewise, also the ablation of *col10a1* cells had no effect on regeneration of osteoblasts and joint cells. Only simultaneous ablation of both cell types slowed down regeneration slightly but did not prevent it. These observations are in line with the existence of osteoblast progenitor cells (OPCs) or tissue founding stem cells (FSCs) that allow *de novo* formation of osteoblasts and joint cells, as proposed in zebrafish (Singh et al., 2012; Tu and Johnson, 2011). Interestingly in zebrafish, these progenitors are located in the intersegmental regions (Ando et al., 2017), where we also identified *col10a1+/osx-* cells.

We employed the Gaudí toolkit, developed initially for tracking retinal stem cells (Centanin et al., 2014), to determine the contribution of *col10a1* cells to the regenerating fin in adult medaka fish. We found that

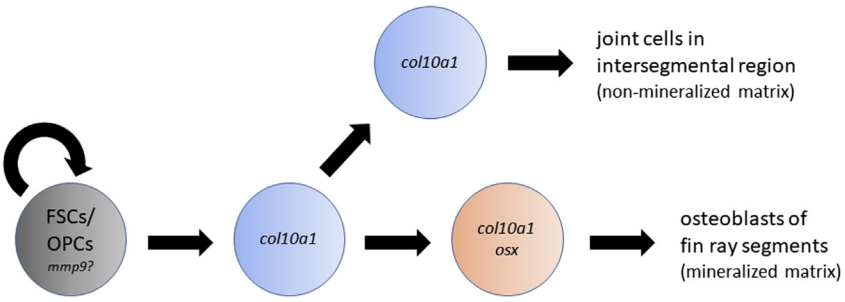

Fig. 9. Model for the role of *col10a1* cells in the regenerating fin. After ablation of mature *osx* positive osteoblasts, founding stem cells (FSCs; Tu and Johnson, 2011) or osteoblast progenitor cells (OPCs) that express *mmp9* in zebrafish (Ando et al., 2017) become activated and differentiate into *col10a1* positive progenitors. A subset of these *col10a1* cells starts to express *osx* and differentiates into osteoblasts that produce the mineralzing matrix of fin ray segments. The residual *col10a1* cells postioned in the intersegmental boundaries persist as *osx* negative cells, become joint cells and produce non-mineralizing matrix.

col10a1 cells at the stump contribute to osteoblasts along segments as well as joint cells in the intersegmental regions. The ablation of *osx* cells completely blocked contribution of *col10a1*+/*osx*- cells to the segment osteoblasts but did not affect their contribution to intersegmental regions. The observation that after *osx* ablation none of the segmental osteoblasts in the regenerate expressed the lineage tracer demonstrated that all segmental osteoblasts in the adult caudal fin express *osx* and were efficiently ablated. It furthermore showed that *col10a1* marks an *osx*--negative cell population that exclusively gives rise to regenerating joint cells. Importantly, other studies showing osteoblast labelling in zebrafish did not report contribution of osteoblasts into joint cells (Knopf et al., 2011; Sousa et al., 2011; Stewart and Stankunas, 2012). We therefore suggest the presence of two distinct cell populations in the fin that are marked by *col10a1* (Fig. 9). Both are non-interconvertible and give rise either to osteoblasts or to joint cells.

We quantified ablation efficiency and found that on average 93% of *osx* cells were ablated using our nitroreductase protocol in medaka. Furthermore, we showed that the remaining cells that had escaped ablation did not exhibit increased proliferation. Thus, while non-ablated cells probably participated in regeneration, it is very unlikely that they contributed significantly to the re-population of the osteoblast pool during regeneration. On the other hand, we can not exclude that *col10a1* negative cells in the joint region, which were not ablated and most likely include OPCs, contributed to regeneration.

4.3. Lineage restricted progenitor pools account for osteoblast regeneration in ablated fins

Under normal regeneration conditions, mature osteoblasts dedifferentiate to generate progenitors that re-differentiate into osteoblasts. However, in the absence of mature osteoblasts (i.e. after ablation) alternative cellular sources are activated to allow regeneration. In principle, two possible mechanisms can account for this *de novo* generation of osteoblasts: Stem/progenitor cell activation and/or transdifferentiation.

Previous studies on random labelling of fin cells employed fin-specific Cre expression (Stewart and Stankunas, 2012) or transposon-based techniques (Tu and Johnson, 2011) to limit the number of labelled cell types. Earlier clonal analysis identified nine discrete cell lineage classes for the zebrafish caudal fin and suggested distinct FSCs for each lineage (Tu and Johnson, 2011). Each of the lineages showed strict fate restriction, and the possibility of transfating or transdifferentiation between lineages was excluded.

Consistently, our data from clonal analysis of randomly labelled cell types also did not show any evidence for transdifferentiation in medaka. We used the Gaudí toolkit to label different progenitor cell pools by Cre induction at embryonic and post-hatching stages (1–15 dpf), and followed their fate after ablation of differentiated osteoblasts and amputation of the fin. These progenitor cells differentiated and gave rise to labelled clones in the adult caudal fin in patterns that were highly similar to those previously reported in zebrafish (Stewart and Stankunas, 2012; Tu and Johnson, 2011). Our results show that after *osx* cell ablation only clones derived from osteoblast progenitors (Type II) contribute to segmental osteoblasts. All other mosaics that lacked Type II labelled cells did not show any labelled osteoblasts in the regenerate. This strongly suggests that also in medaka transdifferentiation does not occur after ablation of differentiated osteoblasts. Instead, we provide the first evidence that when challenged by ablation of mature osteoblasts in medaka, lineage restricted progenitor cells are responsible for the generation of joint cells and osteoblasts in the regenerating fins. Whether these progenitors in medaka behave similarly as the *mmp9* positive OPCs in zebrafish remains to be tested. Importantly, the *col10a1* cells in the intersegmental regions of medaka differ in many aspects from the *mmp9* OPCs described in zebrafish (Ando et al., 2017). First, ablation of *col10a1* cells does not affect fin regeneration and *de novo* osteoblast formation, while ablation of *mmp9* cells does. Secondly, while *mmp9*+ cells contribute to both osteoblasts and joint cells, *col10a1*+ /*osx*- cells in the intersegmental region exclusively contribute to joint cells but not to osteoblasts. We therefore speculate that *col10a1* cells represent immediate derivatives of *mmp9*+ OPCs and are subdivided into two cell populations: One that eventually will become *osx*–positive and will differentiate into segmental osteoblasts producing mineralizing matrix, and a second that remains *osx*-negative and produces the non-mineralizing matrix of the joints (Fig. 9). Which factors trigger the activation of progenitors and control the divergence of both populations remains to be analysed.

Acknowledgements

We thank Ann Huyseunne and P. Eckhard Witten for critical comments and discussions, and Patrick Laurenti for providing the *eve1* plasmid. This project is funded by grants from the Singapore Ministry of Education (MOE, grant numbers 2013-T2-2-126 and 2016-T2-2-086) and the National Research Foundation Singapore (NRF, grant numberNRF2017-NRF-ISF002-2671). M.D. and T.W.H. received graduate scholarships from the National University of Singapore (NUS) Department of Biological Sciences. We thank the confocal unit of the NUS Centre for Bioimaging Sciences (CBIS) for their constant support.

Appendix A. Supplementary data

Supplementary data to this article can be found online at https://doi.org/10.1016/j.ydbio.2019.07.012.

References

Akimenko, M.-A., Mari-Beffa, M., Becerra, J., Geraudie, J., 2003. Old questions, new tools, and some answers to the mystery of fin regeneration. Dev. Dynam. 226, 190–201.

Akimenko, M.A., Johnson, S.L., Westerfield, M., Ekker, M., 1995. Differential induction of four msx homeobox genes during fin development and regeneration in zebrafish. Development 121, 347–357.

Ando, K., Shibata, E., Hans, S., Brand, M., Kawakami, A., 2017. Osteoblast production by reserved progenitor cells in zebrafish bone regeneration and maintenance. Dev. Cell 43, 643–650 e643.

Askary, A., Mork, L., Paul, S., He, X., Izuhara, A.K., Gopalakrishnan, S., Ichida, J.K., McMahon, A.P., Dabizljevic, S., Dale, R., Mariani, F.V., Crump, J.G., 2015. Iroquois proteins promote skeletal joint formation by maintaining chondrocytes in an immature state. Dev. Cell 35, 358–365.

Avaron, F., Hoffman, L., Guay, D., Akimenko, M.A., 2006. Characterization of two new zebrafish members of the hedgehog family: atypical expression of a zebrafish indian

hedgehog gene in skeletal elements of both endochondral and dermal origins. Dev. Dynam. 235, 478–489.
Bateman, J.F., Freddi, S., McNeil, R., Thompson, E., Hermanns, P., Savarirayan, R., Lamande, S.R., 2004. Identification of four novel COL10A1 missense mutations in schmid metaphyseal chondrodysplasia: further evidence that collagen X NC1 mutations impair trimer assembly. Hum. Mutat. 23, 396.
Blum, N., Begemann, G., 2015. Osteoblast de- and redifferentiation are controlled by a dynamic response to retinoic acid during zebrafish fin regeneration. Development 142, 2894–2903.
Borday, V., Thaeron, C., Avaron, F., Brulfert, A., Casane, D., Laurenti, P., Geraudie, J., 2001. evx1 transcription in bony fin rays segment boundaries leads to a reiterated pattern during zebrafish fin development and regeneration. Dev. Dynam. 220, 91–98.
Brockes, J.P., Kumar, A., 2008. Comparative aspects of animal regeneration. Annu. Rev. Cell Dev. Biol. 24, 525–549.
Centanin, L., Ander, J.J., Hoeckendorf, B., Lust, K., Kellner, T., Kraemer, I., Urbany, C., Hasel, E., Harris, W.A., Simons, B.D., Wittbrodt, J., 2014. Exclusive multipotency and preferential asymmetric divisions in post-embryonic neural stem cells of the fish retina. Development 141, 3472–3482.
Dardis, G., Tryon, R., Ton, Q., Johnson, S.L., Iovine, M.K., 2017. Cx43 suppresses evx1 expression to regulate joint initiation in the regenerating fin. Dev. Dynam. 246, 691–699.
Debiais-Thibaud, M., Borday-Birraux, V., Germon, I., Bourrat, F., Metcalfe, C.J., Casane, D., Laurenti, P., 2007. Development of oral and pharyngeal teeth in the medaka (Oryzias latipes): comparison of morphology and expression of eve1 gene. J. Exp. Zool. B Mol. Dev. Evol. 308B (6), 693–708.
Echeverri, K., Clarke, J.D., Tanaka, E.M., 2001. In vivo imaging indicates muscle fiber dedifferentiation is a major contributor to the regenerating tail blastema. Dev. Biol. 236, 151–164.
Flores, M.V., Tsang, V.W., Hu, W., Kalev-Zylinska, M., Postlethwait, J., Crosier, P., Crosier, K., Fisher, S., 2004. Duplicate zebrafish runx2 orthologues are expressed in developing skeletal elements. Gene Expr. Patterns 4, 573–581.
Haas, H.J., 1962. Studies on mechanisms of joint and bone formation in the skeleton rays of fish fins. Dev. Biol. 5, 1–34.
Hay, E.D., Fischman, D.A., 1961. Origin of the blastema in regenerating limbs of the newt Triturus viridescens. An autoradiographic study using tritiated thymidine to follow cell proliferation and migration. Dev. Biol. 3, 26–59.
Ito, K., Morioka, M., Kimura, S., Tasaki, M., Inohaya, K., Kudo, A., 2014. Differential reparative phenotypes between zebrafish and medaka after cardiac injury. Dev. Dynam. 243, 1106–1115.
Johnson, S.L., Bennett, P., 1999. Growth control in the ontogenetic and regenerating zebrafish fin. Methods Cell Biol. 59, 301–311.
Khmelinskii, A., Keller, P.J., Bartosik, A., Meurer, M., Barry, J.D., Mardin, B.R., Kaufmann, A., Trautmann, S., Wachsmuth, M., Pereira, G., Huber, W., Schiebel, E., Knop, M., 2012. Tandem fluorescent protein timers for in vivo analysis of protein dynamics. Nat. Biotechnol. 30, 708–714.
Knopf, F., Hammond, C., Chekuru, A., Kurth, T., Hans, S., Weber, C.W., Mahatma, G., Fisher, S., Brand, M., Schulte-Merker, S., Weidinger, G., 2011. Bone regenerates via dedifferentiation of osteoblasts in the zebrafish fin. Dev. Cell 20, 713–724.
Konig, D., Page, L., Chassot, B., Jazwinska, A., 2017. Dynamics of actinotrichia regeneration in the adult zebrafish fin. Dev. Biol. 433 (2), 416–432.
Kragl, M., Knapp, D., Nacu, E., Khattak, S., Maden, M., Epperlein, H.H., Tanaka, E.M., 2009. Cells keep a memory of their tissue origin during axolotl limb regeneration. Nature 460, 60–65.
Lai, S.L., Marin-Juez, R., Moura, P.L., Kuenne, C., Lai, J.K.H., Tsedeke, A.T., Guenther, S., Looso, M., Stainier, D.Y., 2017. Reciprocal analyses in zebrafish and medaka reveal that harnessing the immune response promotes cardiac regeneration. Elife 6.
Li, N., Felber, K., Elks, P., Croucher, P., Roehl, H.H., 2009. Tracking gene expression during zebrafish osteoblast differentiation. Dev. Dynam. 238, 459–466.
Lo, D.C., Allen, F., Brockes, J.P., 1993. Reversal of muscle differentiation during urodele limb regeneration. Proc. Natl. Acad. Sci. U. S. A. 90, 7230–7234.
Lust, K., Wittbrodt, J., 2018. Activating the regenerative potential of Muller glia cells in a regeneration-deficient retina. Elife 7.
McIntosh, I., Abbott, M.H., Francomano, C.A., 1995. Concentration of mutations causing Schmid metaphyseal chondrodysplasia in the C-terminal noncollagenous domain of type X collagen. Hum. Mutat. 5, 121–125.
McMillan, S.C., Zhang, J., Phan, H.E., Jeradi, S., Probst, L., Hammerschmidt, M., Akimenko, M.A., 2018. A Regulatory Pathway Involving Retinoic Acid and Calcineurin Demarcates and Maintains Joint Cells and Osteoblasts in Regenerating Fin, vol.145. Development.
Nye, H.L., Cameron, J.A., Chernoff, E.A., Stocum, D.L., 2003. Regeneration of the urodele limb: a review. Dev. Dynam. 226, 280–294.
Poleo, G., Brown, C.W., Laforest, L., Akimenko, M.A., 2001. Cell proliferation and movement during early fin regeneration in zebrafish. Dev. Dynam. 221, 380–390.
Rembold, M., Lahiri, K., Foulkes, N.S., Wittbrodt, J., 2006. Transgenesis in fish: efficient selection of transgenic fish by co-injection with a fluorescent reporter construct. Nat. Protoc. 1, 1133–1139.
Renn, J., Winkler, C., 2009. Osterix-mCherry transgenic medaka for in vivo imaging of bone formation. Dev. Dynam. 238, 241–248.
Renn, J., Buttner, A., To, T.T., Chan, S.J., Winkler, C., 2013. A col10a1:nlGFP transgenic line displays putative osteoblast precursors at the medaka notochordal sheath prior to mineralization. Dev. Biol. 381, 134–143.
Renn, J., Winkler, C., 2012. Osterix:nlGFP transgenic medaka identify regulatory roles for retinoic acid signaling during osteoblast differentiation in vivo. J. Appl. Ichthyol. 28, 360–363.
Sandoval-Guzman, T., Wang, H., Khattak, S., Schuez, M., Roensch, K., Nacu, E., Tazaki, A., Joven, A., Tanaka, E.M., Simon, A., 2014. Fundamental differences in dedifferentiation and stem cell recruitment during skeletal muscle regeneration in two salamander species. Cell Stem Cell 14, 174–187.
Santamaria, J.A., Becerra, J., 1991. Tail fin regeneration in teleosts: cell-extracellular matrix interaction in blastemal differentiation. J. Anat. 176, 9–21.
Schindelin, J., Arganda-Carreras, I., Frise, E., Kaynig, V., Longair, M., Pietzsch, T., Preibisch, S., Rueden, C., Saalfeld, S., Schmid, B., Tinevez, J.Y., White, D.J., Hartenstein, V., Eliceiri, K., Tomancak, P., Cardona, A., 2012. Fiji: an open-source platform for biological-image analysis. Nat. Methods 9, 676–682.
Sims Jr., K., Eble, D.M., Iovine, M.K., 2009. Connexin 43 regulates joint location in zebrafish fins. Dev. Biol. 327, 410–418.
Singh, S.P., Holdway, J.E., Poss, K.D., 2012. Regeneration of amputated zebrafish fin rays from de novo osteoblasts. Dev. Cell 22, 879–886.
Smith, A., Avaron, F., Guay, D., Padhi, B.K., Akimenko, M.A., 2006. Inhibition of BMP signaling during zebrafish fin regeneration disrupts fin growth and scleroblasts differentiation and function. Dev. Biol. 299, 438–454.
Sousa, S., Afonso, N., Bensimon-Brito, A., Fonseca, M., Simoes, M., Leon, J., Roehl, H., Cancela, M.L., Jacinto, A., 2011. Differentiated skeletal cells contribute to blastema formation during zebrafish fin regeneration. Development 138, 3897–3905.
Stewart, S., Stankunas, K., 2012. Limited dedifferentiation provides replacement tissue during zebrafish fin regeneration. Dev. Biol. 365, 339–349.
Straube, W.L., Tanaka, E.M., 2006. Reversibility of the differentiated state: regeneration in amphibians. Artif. Organs 30, 743–755.
Ton, Q.V., Iovine, M.K., 2013. Identification of an evx1-dependent joint-formation pathway during FIN regeneration. PLoS One 8, e81240.
Tu, S., Johnson, S.L., 2010. Clonal analyses reveal roles of organ founding stem cells, melanocyte stem cells and melanoblasts in establishment, growth and regeneration of the adult zebrafish fin. Development 137, 3931–3939.
Tu, S., Johnson, S.L., 2011. Fate restriction in the growing and regenerating zebrafish fin. Dev. Cell 20, 725–732.
Willems, B., Buttner, A., Huysseune, A., Renn, J., Witten, P.E., Winkler, C., 2012. Conditional ablation of osteoblasts in medaka. Dev. Biol. 364, 128–137.
Yoshinari, N., Ishida, T., Kudo, A., Kawakami, A., 2009. Gene expression and functional analysis of zebrafish larval fin fold regeneration. Dev. Biol. 325, 71–81.